Osteoarthritis and Cartilage Open 4 (2022) 100295

Contents lists available at ScienceDirect

Osteoarthritis and Cartilage Open

journal homepage: www.elsevier.com/journals/osteoarthritis-and-cartilage-open/2665-9131

Synovial tissue metabolomic profiling reveal biomarkers of synovial inflammation in patients with osteoarthritis

Jessica D. Murillo-Saich [a], Roxana Coras [a,b], Robert Meyer [a,c], Cristina Llorente [a], Nancy E. Lane [d], Monica Guma [a,b,c,*]

[a] Department of Medicine, School of Medicine, University of California, San Diego, 9500 Gilman Drive, San Diego, CA, 92093, USA
[b] Department of Medicine, Autonomous University of Barcelona, Plaça Cívica, 08193 Bellaterra, Barcelona, Spain
[c] San Diego VA Healthcare Service, San Diego, CA, 92161, USA
[d] Department of Medicine, University of California, Davis, Sacramento, CA, 95817, USA

ARTICLE INFO

Keywords:
Inflammation
Fibrosis
Metabolomic
Synovial fluid

ABSTRACT

Objective: Inflammatory responses are associated with changes in tissue metabolism. Prior studies find altered metabolomic profiles in both the synovial fluid (SF) and serum of osteoarthritis subjects. Our study determined the metabolomic profile of synovial tissue (ST) and SF of individuals with osteoarthritis (OA) and its association with synovial inflammation.

Design: 37 OA ST samples were collected during joint replacement, 21 also had SF. ST samples were fixed in formalin for histological analysis, cultured (explants) for cytokine analysis by enzyme-linked immunosorbent assay, or snap-frozen for metabolomic analysis. ST samples were categorized by Krenn synovitis score and picrosirius red. CD68 and vimentin expression was assessed by immunohistochemistry and semi-quantified using Image J. Proton-nuclear magnetic resonance (^{1}H NMR) was used to acquire a spectrum from ST and SF samples. Chenomx NMR suite 8.5 was used for metabolite identification and quantification. Metaboanalyst 5.0, SPSS v26, and R (v4.1.2) were used for statistical analysis.

Results: 42 and 29 metabolites were detected in the ST and SF respectively by ^{1}H NMR. Only 3 metabolites, lactate, dimethylamine, and creatine positively correlated between SF and ST. ST concentrations of several metabolites (lactate, alanine, fumarate, glutamine, glycine, leucine, lysine, methionine, trimethylamine *N*-oxide, tryptophan and valine) were associated with synovitis score, mostly to the lining score. IL-6, acetoacetate, and tyrosine in SF predicted high Krenn synovitis scores in ST.

Conclusion: Metabolomic profiling of ST identified metabolic changes associated with inflammation. Further studies are needed to determine whether metabolomic profiling of synovial tissue can identify new therapeutic targets in osteoarthritis.

1. Introduction

Osteoarthritis (OA) is the most common form of arthritis and one of the leading causes of impaired mobility among older adults [1]. The synovium in OA patients is characterized by synovial lining hyperplasia, a sublining with mononuclear and fibroblast cell infiltration, fibrosis, and stromal vascularization [2]. Macrophages are shown to be the most predominant immune cells in OA synovium. Macrophages are believed to play a critical role in OA pathogenesis through the induction of inflammatory mediators, growth factors, and proteinases [3–5].

Synovial fibrosis, which is characterized by fibroblast hyperplasia and an imbalance between synthesis and degradation of collagens, is also a hallmark of OA [6]. It leads to thickening and stiffening of the synovial membrane, which is believed to be a major contributor to both joint pain and joint stiffness. Macrophages and fibroblast-like synoviocytes (FLS) react to molecules from degraded hyaline cartilage by producing pro-inflammatory mediators and fibrotic mediators. These in turn act on both synoviocytes and chondrocytes to not only produce excess of proteolytic enzymes that augment cartilage degradation, but also generate additional inflammatory mediators to further amplify synovial inflammation and fibrosis [7].

Increasing evidence indicate that synovial inflammation [8]

* Corresponding author. Department of Medicine, School of Medicine, University of California, San Diego, 9500 Gilman Drive, San Diego, CA, 92093, USA.
E-mail address: mguma@health.ucsd.edu (M. Guma).

https://doi.org/10.1016/j.ocarto.2022.100295
Received 25 June 2022; Received in revised form 4 July 2022; Accepted 5 July 2022

contributes to OA progression [6]. Synovitis can occur prior to incident radiographic OA, and effusion synovitis 1–2 years prior to diagnosis is significantly associated with subsequent OA development [9,10]. These results suggest that inflammation is a part of the spectrum of OA pathology.

Metabolism is important for cartilage and synovial joint function [11]. Metabolic changes from a resting regulatory state to an active metabolic state both in chondrocytes and synoviocytes were reported in OA and implicated in its pathogenesis [11,12]. One of these metabolic changes is the upregulation of the glycolytic cycle due to the increased demand in energy and the activation of glucose transporters in response to hypoxia and proinflammatory cytokines, resulting in increased concentration of glucose, lactate and pyruvate, among others [11,12]. Emerging evidence indicates an important role for metabolites derived from key metabolic pathways in the regulation of inflammatory responses and cell function. Glucose and choline metabolism, for instance, support the expression of proinflammatory cytokines [13–17], while tryptophan, and derivates of fumarate have been associated to an anti-inflammatory role [18]. Other metabolites have mixed properties, like succinate, a metabolite that supports inflammation but also has immunomodulatory functions [19].

Previous studies have shown metabolomic alterations in OA in different biofluids such as urine [20], synovial fluid (SF) [21,22], blood serum [23], and plasma [24], determined by nuclear magnetic resonance (NMR) or mass spectrometry. However, a metabolomic characterization of the OA synovial tissue and their association with histological features and association with synovial fluid metabolomics has not been performed. This study determined the metabolomic profile in SF to predict inflammation of ST in individuals with OA.

2. Method

Patients: Thirty-seven synovial tissue (ST) samples with twenty-one paired synovial fluid (SF) samples were obtained during joint replacement in patients diagnosed with hip and knee OA [25] at the Veterans Affairs (VA) San Diego Health Care System. Age and sex were also collected. ST samples were obtained from the suprapatellar area (knee) and from the inferior capsular region (hip). The samples were kept on ice until they were fixed in formalin for histological analysis, cultured (explants) for 24 h for cytokine analysis by enzyme-linked immunosorbent assay (ELISA), or snap-frozen for metabolomic analysis. SF samples collected the same day were centrifuged at 4000 rpm for 10 min, cells were discarded, and supernatant was stored at −80 °C. Patients signed and informed consent and the protocol was approved by the VA Institutional Review Board (IRB number H170130). The study was conducted in accordance with the Helsinki Declaration of 1975, as revised in 2000.

Histology: ST samples were fixed in formalin 10% (Thermo scientific, #5735) and embedded in paraffin. ST (5 μM) were stained using Hematoxylin and Eosin (H&E), and synovitis was evaluated according to the Krenn histopathological synovitis score [26]. Based on the Krenn score, ST samples were classified as low (score 0–4) or high (score 5–9) degree synovitis. Synovial lining and sublining infiltration (identified with H&E) were scored using a semiquantitative method from 0 to 3 and were grouped as low (<2) or high (≥ 2) scores. The slides were scored by two different researchers using the microscope Motic BA400. Fibrosis was identified with picrosirius red staining. The picrosirius red staining highlights the natural birefringence of collagen fibers when exposed to polarized light. This allows evaluating the organization of collagen fibers in the tissues and the semiquantification of type I and III collagen, identifying fibers type I in red and type III in green [27,28]. Fibrosis was scored using a semiquantitative scoring from 0 to 3 and were grouped as low collagen (<2) or high collagen (≥ 2) scores.

Immunohistochemistry (IHC): IHC was used to quantify macrophages and fibroblasts in the ST samples. IHC analysis was performed using 5 μM sections of formalin-fixed paraffin-embedded ST samples. After deparaffinization and rehydration, antigen retrieval was performed by boiling in citrate buffer pH 6 for 10 min with pressure cooker. Next, endogenous peroxidase was inactivated with 3% H_2O_2 in water for 10 min at room temperature. Sections were incubated with 3% BSA (bovine serum albumin) for 1 h at room temperature, and then with the specific primary antibody overnight at 4 °C. After washing, the secondary antibody was added for 30 min at room temperature and sections were washed three times with PBS. 3,30-Diaminobenzidinetetrahydrochloride (DAB) (Vector, #SK-4100) was used as a chromogen. Sections were lightly counterstained with hematoxylin, dehydrated and then mounted. A non-related IgG was used as a negative control. The antibodies and working concentrations used are listed below.

- CD68. Abcam#ab955 1/500 (Clone KP1)
- Vimentin. Cell Signaling #D2H13 1/100

The slides were scanned using a NanoZoomer slide scanner using a 40x brightfield objective. Semiquantitative determination of antibody expression was performed using Image J Fiji, according to the method described by Alexander Crowe et al. [29] IHC images stained with hematoxylin and DAB were deconvoluted and the expression of CD68 and vimentin were calculated using a threshold for DAB of 170.

Metabolite extraction from synovial tissue: Metabolite extraction of ST samples was performed using a protein precipitation protocol. Approximately 14 mg of each sample was snap-frozen and stored at −80 °C before metabolite extraction. The tissue was ground with a hydroalcoholic mix using Beadblaster microtube homogenizer. Next, chloroform was added then shaken for 1 min. The samples were centrifuged for 5 min at 1200 rpm to separate the polar layer which contains the polar metabolites. This was evaporated using a speed vacuum (Thermo Fisher Scientific, Waltham, MA) and the metabolites were resuspended in 60 μL of the standard 3-(Trimethylsilyl) propioninc-2,2,3,3,d_4 acid sodium salt (TSP-d4) (Millipore Sigma, Cat#269913) at a concentration of 66.17 μM. Then, 50 μL of each sample was added into a 1.7 mm BioSpin tube.

Metabolite extraction from synovial fluid: The SF samples were thawed on ice and polar metabolites were extracted using an ultrafiltration method with a 3 KDa filter device with 30 min of centrifugation at 12,000 rpm, 4 °C. Then, 45 μL were taken from the filtered sample and 15 μL of TSP-d4 standard 2 mM were added to obtain a final concentration of 0.5 mM. Finally, 50 μL of each sample were added into a 1.7 mm BioSpin tube.

Data acquisition, identification, and quantification of metabolites: A 600 MHz Bruker Avance III spectrometer one-dimension proton-nuclear magnetic resonance (^{1}H NMR) was used to acquire NMR spectra of ST and SF samples. The standard Bruker pulse sequence "noesygppr1d" was used with a mixing time of 500 ms and 64 scans. A daily quality assurance procedure was performed before sample data acquisition, involving temperature checks and calibration as well as shim and water suppression quality. The data acquisition was obtained in the NMR facility of Skaggs School of Pharmacy and Pharmaceutical Science, University of California San Diego. Software Chenomx NMR suite 8.5 professional was used for metabolite identification and quantification. Samples were normalized by vol/wt and the concentrations were reported in μM.

Quantification of inflammatory mediators in explants and SF samples: Explants (around 15 mg) were cultured in triplicates with complete media (Gibco Dubbeco's modified eagle medium #11965 with 10% fetal bovine serum (FBS), 1% glutamine, 1% pen strep and gentamicin). Supernatants were collected after 24 h and stored at −20 °C for cytokine analysis. SF samples were collected and centrifuged at 4000 rpm for 10 min, cells were discarded, and the supernatant was stored at −80 °C before analysis. Interleukin 6 (IL-6) (R&D, DY206), Interleukin 1 beta (IL-1β) (R&D, #DY201), Tumor necrosis factor (TNF) (R&D, #DY210), C-X-C Chemokine ligand 2 (CXCL2) (R&D, #DY452), C–C Motif Chemokine Ligand 2 (CCL2) (R&D, #DY279), and Matrix metallopeptidase 13 (MMP13) (R&D, #DY511) were measured in both explant supernatants and SF samples by ELISA following manufacturers' instructions.

Statistical analysis: Continuous variables are shown in mean ± standard deviation (SD) and categorical variables are shown in percentages. Student *t*-test was used to evaluate the differences between quantitative clinical variables, concentration of cytokines, and metabolites between 2 groups, Differences between categorical variables were assessed using Chi-square with SPSS software v27. We also performed orthogonal partial least square discrimination analysis (OPLS-DA) and the variables important of projection (VIP) was performed to identify the metabolites that contribute to separation between different groups using MetaboAnalyst v5. The strength of association between metabolites presented in synovial tissue and synovial fluid, and between metabolites and cytokines was measured with Pearson correlation using "gplots" package (https://cran.r-project.org/web/packages/gplots/gplots.pdf). To identify if SF features (metabolites and cytokines) that could predict the degree of synovitis (high versus low), a Random Forest predictive model was implemented using the "randomForest" package (https://cran.r-project.org/web/packages/randomForest/index.html). Boruta feature selection was first performed using the Boruta package (https://cran.r-project.org/web/packages/Boruta/index.html) with maximum runs set at 250. The data was next partitioned in training (50% of the data) and testing (50% of the data) datasets, and the Random Forest was built including only the metabolites selected by the Boruta algorithm. Next, the predictive ability of the model was evaluated using a receiver operation curve (ROC) analysis using the 21 samples with SF (https://cran.r-project.org/web/packages/pROC/index.html).

3. Results

3.1. Histological classification of ST samples

A total of 37 synovial tissue (ST) samples were obtained from 28 knees and 9 hips. The average age of the individuals with OA was 66 ± 8.5 and 86.5% were men. ST samples were classified as either low (n = 22) or high (n = 15) synovitis scores by H&E staining, and as either low (n = 18) or high (n = 19) fibrosis scores by picrosirius red staining (Fig. 1 and Supplementary Table 1). Age and sex were not different between synovitis or fibrosis categories. Although all samples have both inflammation and fibrosis features, the highly inflamed samples showed less fibrosis and vice versa (Supplementary Table 2). Interestingly, hip samples tended to be more fibrotic than inflammatory, while knees shared both inflammation and fibrotic characteristics (Supplementary Table 2). Both collagens (type I and III) were more abundant in high fibrotic tissue, and the collagen I/III ratio was similar in all groups (Table 1, Supplementary Table 1).

We also stained the synovial tissue with CD68 and vimentin to determine the abundance and distribution of macrophages and fibroblasts in the synovium, respectively (Fig. 1). Although not significant, in knees we observed an increased expression of CD68 (0.84 ± 1.23 vs 1.35 ± 1.18, p = 0.17) and vimentin (1.59 ± 1.40 vs 3.23 ± 5.79, p = 0.32) in inflamed tissues. Interestingly, when we compared the location of the abundance of these two cellular markers, we observed a tendency for higher expression of vimentin in the sublining of high synovitis samples (1.71 ± 0.73 vs 2.07 ± 0.51, p = 0.14), but not in the high fibrotic samples (2.00 ± 0.59 vs 1.78 ± 0.70, p = 0.39) (Table 1 and Supplementary Table 1).

3.2. Metabolomic profile of synovial tissue in inflamed and non-inflamed synovial samples

A total of 42 metabolites were detected in ST samples by ^{1}H NMR. Multivariate approaches were conducted to capture the global picture of 2 metabolite disturbances according to the degree of synovitis. Using an OPLS-DA with all identified metabolites, 52.6% of the total variance across groups explained the separation. As observed in Supplementary Figure 1A, this approach was able to discriminate the two groups analyzed including hips and knees, although a certain overlap existed. A total of 14 metabolites had VIP scores >1 (Supplementary Figure 1B). Glucose was identified as the most important metabolite to discriminate between low and high synovitis, followed by glycine, dimethyl sulfone, dimethylamine, acetate, acetone and tryptophan. When only knees were included, glucose was also identified as the most important metabolite and no major differences were observed (Supplementary Fig. 1C and D). We also performed an OPLS-DA according to fibrosis groups (Supplementary Figure 1E). 54.2% Of the total variance across groups was explained and a total of 13 metabolites had VIP scores >1 including hips and knees, *o*-phosphoethanolamine, acetoacetate, glucose, glutamine,

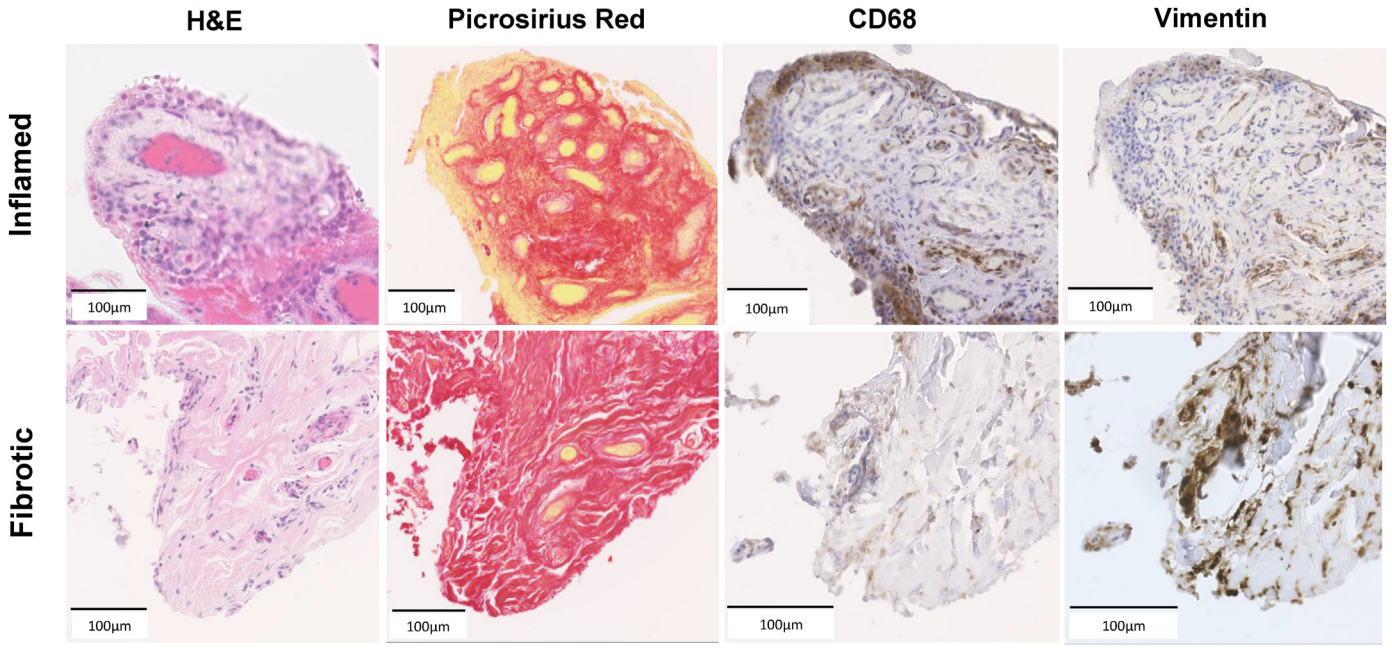

Fig. 1. Histological classification of synovial tissue from osteoarthritis (OA) patients in inflamed (upper panels) or fibrotic (bottom panel) samples. Hematoxylin Eosin staining of synovial tissue, Picrosirius red staining on red the collagen fibers, immunohistochemistry (IHC) for CD68 as marker of macrophages and IHC for Vimentin as marker of fibroblasts.

Table 1
Comparison of histological characteristics according to inflammation and fibrosis in knee samples.

Variables	Inflammation		P	Fibrosis		P
	Low synovitis N = 14	High synovitis N = 14		Low collagen N = 14	High collagen N = 14	
Age, years	66.14 ± 6.12	68.35 ± 4.57	0.28	68.57 ± 4.36	65.93 ± 6.18	0.20
Male, n (%)	13 (92.9)	13 (92.9)	1.00	12 (85.7)	14 (100)	0.48
CD68	0.84 ± 1.23	1.35 ± 1.18	0.17	1.69 ± 2.32	0.97 ± 1.23	0.31
CD68 Lining	0.89 ± 1.05	1.36 ± 1.18	0.28	1.36 ± 1.13	0.89 ± 1.11	0.28
CD68 Sublining	1.00 ± 0.64	0.96 ± 0.41	0.86	0.93 ± 0.43	1.03 ± 0.63	0.61
Vimentin	1.59 ± 1.40	3.23 ± 5.79	0.32	3.11 ± 5.81	1.71 ± 1.44	0.39
Vimentin Lining	1.28 ± 1.15	1.75 ± 0.84	0.24	1.86 ± 0.77	1.18 ± 1.15	**0.07**
Vimentin Sublining	1.71 ± 0.73	2.07 ± 0.51	0.14	2.00 ± 0.59	1.78 ± 0.70	0.39
Total Collagen	1.96 ± 0.60	1.32 ± 0.61	**0.009**	1.07 ± 0.38	2.21 ± 0.32	< **0.001**
Collagen type I	1.68 ± 0.64	1.21 ± 0.75	0.09	0.96 ± 0.49	1.93 ± 0.58	< **0.001**
Collagen type III	1.39 ± 0.52	0.96 ± 0.46	**0.03**	0.96 ± 0.46	1.39 ± 0.52	**0.03**
Collagen I/III	1.36 ± 0.70	1.40 ± 0.87	0.87	1.15 ± 0.73	1.61 ± 0.77	0.12

Quantitative variables are expressed in mean ± standard deviation and qualitative variables are expressed in count and percentage. Student *t*-test was used to compared quantitative variables and, Chi square for qualitative variables. Considering inflammation low synovitis <5 and high synovitis ≥5 according to Krenn score. Fibrosis low collagen <2, high collagen ≥2 according to picrosirius red staining.

Table 2
Comparison of polar metabolites detected by 1H NMR in synovial tissue of knee samples between inflammation and fibrosis groups.

Variables	Inflammation		P	Fibrosis		p
	Low synovitis N = 14	High synovitis N = 14		Low collagen N = 14	High collagen N = 14	
3-Hydroxybutyrate	0.62 ± 0.58	0.75 ± 0.63	0.59	0.81 ± 0.65	0.55 ± 0.53	0.25
Acetate	17.14 ± 14.33	15.27 ± 14.47	0.73	15.29 ± 14.23	17.12 ± 14.57	0.74
Acetoacetate	0.14 ± 0.10	0.22 ± 0.13	0.07	0.21 ± 0.14	0.15 ± 0.09	0.20
Acetone	0.09 ± 0.06	0.07 ± 0.04	0.16	0.08 ± 0.04	0.09 ± 0.07	0.76
Alanine	4.09 ± 1.78	6.17 ± 2.93	**0.03**	6.35 ± 2.73	3.91 ± 1.85	**0.01**
Betaine	0.38 ± 0.28	0.38 ± 0.24	0.96	0.46 ± 0.29	0.30 ± 0.19	0.10
Choline	1.54 ± 0.95	2.04 ± 1.02	0.19	2.10 ± 0.94	1.48 ± 0.99	0.10
Citrate	1.08 ± 0.37	1.37 ± 0.53	0.11	1.39 ± 0.49	1.06 ± 0.40	0.06
Creatine	1.12 ± 0.96	1.25 ± 0.46	0.66	1.47 ± 0.92	0.90 ± 0.37	**0.04**
Creatine phosphate	0.28 ± 0.12	0.40 ± 0.19	0.06	0.37 ± 0.16	0.31 ± 0.18	0.37
Creatinine	0.28 ± 0.26	0.30 ± 0.22	0.77	0.31 ± 0.21	0.27 ± 0.27	0.68
Dimethylamine	0.16 ± 0.10	0.11 ± 0.05	0.12	0.12 ± 0.07	0.14 ± 0.10	0.57
Dimethyl sulfone	0.12 ± 0.15	0.16 ± 0.22	0.57	0.18 ± 0.23	0.11 ± 0.14	0.32
Formate	19.24 ± 12.17	20.73 ± 11.02	0.74	20.57 ± 10.87	19.41 ± 12.34	0.79
Fumarate	0.17 ± 0.10	0.27 ± 0.13	**0.02**	0.26 ± 0.11	0.18 ± 0.12	0.06
Glucose	9.53 ± 3.68	7.47 ± 6.05	0.29	8.24 ± 6.05	8.77 ± 3.96	0.79
Glutamate	7.35 ± 3.76	11.17 ± 6.25	0.06	11.11 ± 5.88	7.41 ± 4.39	0.07
Glutamine	2.55 ± 1.67	4.75 ± 2.81	**0.02**	5.13 ± 2.73	2.17 ± 1.04	**0.001**
Glycine	2.30 ± 2.65	5.43 ± 4.67	**0.04**	5.41 ± 4.91	2.29 ± 2.19	**0.04**
Isoleucine	0.62 ± 0.38	1.00 ± 0.44	**0.02**	1.06 ± 0.41	0.56 ± 0.34	**0.002**
Lactate	28.34 ± 14.98	44.46 ± 21.66	**0.03**	44.47 ± 21.63	28.36 ± 15.00	**0.03**
Leucine	2.00 ± 1.12	2.73 ± 1.10	0.09	2.97 ± 1.02	1.76 ± 0.97	**0.003**
Lysine	2.43 ± 1.27	3.14 ± 1.61	0.20	3.37 ± 1.49	2.20 ± 1.23	**0.03**
Methanol	5.94 ± 6.65	45.22 ± 140.14	0.30	45.42 ± 140.07	5.74 ± 6.79	0.30
Methionine	0.40 ± 0.27	0.67 ± 0.45	0.07	0.69 ± 0.44	0.38 ± 0.25	**0.03**
Myo-Inositol	7.59 ± 6.57	11.48 ± 5.82	0.11	12.97 ± 6.04	6.10 ± 4.83	**0.003**
O-Acetylcarnitine	0.23 ± 0.25	0.32 ± 0.21	0.31	0.31 ± 0.22	0.24 ± 0.24	0.40
OPhosphocholine	0.75 ± 0.41	1.24 ± 0.71	**0.04**	1.27 ± 0.68	0.72 ± 0.42	**0.02**
OPhosphoethanolamine	2.26 ± 1.22	3.69 ± 3.02	0.15	4.26 ± 2.64	1.63 ± 1.01	**0.006**
Oxypurinol	9.76 ± 7.92	14.88 ± 10.46	0.16	14.57 ± 10.38	10.07 ± 8.22	0.21
Phenylalanine	0.69 ± 0.43	0.98 ± 0.51	0.12	1.06 ± 0.50	0.61 ± 0.36	**0.01**
Proline	3.33 ± 1.57	3.97 ± 1.59	0.29	4.21 ± 1.51	3.09 ± 1.49	0.06
Pyruvate	0.23 ± 0.08	0.31 ± 0.17	0.10	0.30 ± 0.16	0.24 ± 0.10	0.20
Sarcosine	0.36 ± 0.22	0.46 ± 0.31	0.37	0.50 ± 0.31	0.32 ± 0.19	0.08
SG3PCh	0.60 ± 0.34	0.70 ± 0.35	0.43	0.78 ± 0.36	0.52 ± 0.29	**0.05**
Succinate	0.73 ± 0.41	0.58 ± 0.26	0.26	0.64 ± 0.28	0.66 ± 0.41	0.86
Threonine	1.43 ± 1.04	1.82 ± 0.90	0.30	2.04 ± 0.88	1.20 ± 0.90	**0.02**
Trimethylamine	0.05 ± 0.03	0.08 ± 0.09	0.24	0.08 ± 0.09	0.05 ± 0.03	0.21
TMNO	0.25 ± 0.23	0.43 ± 0.25	0.06	0.47 ± 0.29	0.21 ± 0.11	**0.007**
Tryptophan	0.44 ± 0.15	0.43 ± 0.25	0.91	0.49 ± 0.23	0.35 ± 0.07	0.20
Tyrosine	0.99 ± 0.50	1.32 ± 0.66	0.14	1.39 ± 0.63	0.92 ± 0.47	**0.03**
Uridine	1.04 ± 0.56	1.43 ± 0.87	0.09	1.47 ± 0.86	0.99 ± 0.54	0.09
Valine	1.74 ± 0.81	2.39 ± 1.12	**0.01**	2.54 ± 1.08	1.59 ± 0.70	**0.01**

Quantitative variables are expressed in mean ± standard deviation. Student t-test was used to compare quantitative variables. Low synovitis <5 and high synovitis ≥5 according to Krenn scor. Low collagen <2, high collagen ≥2 according to picrosirius red staining. SG3PCh: sn-*glycero*-3-phosphocholine; TMNO: Trimethylamine *N*-oxide. Statistical difference was considered when $p < 0.05$. Concentrations are reported in μM.

tyrosine, and phenylalanine among them (Supplementary Figure 1F). When only knees were analyzed, we observed a good separation between low and high collagen (Supplementary Figure 1G), and glutamine followed by isoleucine, leucine, phenylalanine, threonine, and glucose were

the most important metabolites for the separation (Supplementary Figure 1H).

To determine the significantly different metabolites between groups, metabolites were analyzed by univariate analysis. When we analyzed the knees, lactate levels were increased in samples with high synovitis scores (28.34 ± 14.98 vs 44.46 ± 21.66, p = 0.03), as expected. Other metabolites including alanine (4.09 ± 1.78 vs 6.17 ± 2.93, p = 0.03), fumarate (0.17 ± 0.10 vs 0.27 ± 0.13, P = 0.02), glutamine (2.55 ± 1.67 vs 4.75 ± 2.81, p = 0.02), glycine (2.30 ± 2.65 vs 5.43 ± 4.67, p = 0.04), isoleucine (0.62 ± 0.38 vs 1.00 ± 0.44, p = 0.02), *o*-phosphocholine (0.75 ± 0.41 vs 1.24 ± 0.71, p = 0.04) and valine (1.74 ± 0.81 vs 2.39 ± 1.12, p = 0.01) were also significantly elevated in these samples (Table 2 and Supplementary Table 3). Consistently, concentration of 18 metabolites were decreased in high fibrotic ST samples (Table 2 and Supplementary Table 3). Differences in metabolites between hips and knees were also observed (Supplementary Table 4). Of note, the metabolic changes were driven mostly by the lining, as we did not observe many differences when samples were stratified by sublining scores (Supplementary Tables 5 and 6).

3.3. Correlation between synovial fluid and synovial tissue metabolic profiles

^{1}H NMR analysis of SF obtained from 21 knee OA samples identified 29 of the 42 metabolites identified in tissue (Fig. 2). Several metabolites identified in ST including tryptophan, hydroxybutyrate, and betaine among others, were not identified in the paired SF. Correlation analysis between the SF and ST metabolites showed that lactate, dimethylamine, and creatine were positively correlated while formate, acetate, and valine had a negative correlation between ST and SF samples (Fig. 3 and Supplementary Figure 2).

3.4. Inflammatory mediators and metabolites in synovial tissue and synovial fluid reflect tissue histologic features

To determine the relationship between metabolites, proinflammatory mediators, and histologic features, we quantified the levels of TNF, IL-6, IL-1β, CXCL2, CCL2 and MMP13 from synovial explants and SF by ELISA. Concentrations of these mediators were not significantly different between samples with high or lower synovitis, although IL-6 concentration was higher in explants with high synovitis (33,045 ± 35,699 vs 59,447 ± 52,096, p = 0.15) and significantly lower in explants from fibrotic samples (64,045 ± 49,708 vs 20,411 ± 20,160, p = 0.01) (Table 3). In SF, levels of IL-6 (190.8 ± 140.9 vs 639.6 ± 602.6, p = 0.06) and MMP13 (119.2 ± 109.05 vs 434.1 ± 378.2, p = 0.04) were elevated in samples with high synovitis (Table 3). Consistent with their histological characteristics, knees presented higher concentrations of IL-6 (15820.01 ± 28631.64 vs 55669.32 ± 44908.33, p = 0.04), CXCL2 (568.21 ± 684.17 vs 2219.42 ± 1886.67, p = 0.04) and CCL2 (388.04 ± 329.18vs 1652.59 ± 1564.30, p = 0.008) (Supplementary Table 7).

The correlation between pro-inflammatory mediators and metabolites showed that IL-6 in explants was positively associated with several metabolites, including alanine, betaine, fumarate, glutamine, glycine, leucine, lysine, methionine, myo-inositol, O-phosphocholine, *o*-phosphoethanolamine, phenylalanine, TMNO, tryptophan, tyrosine, uridine and valine. In addition, TNF and CXCL2 from explants correlated with ST TMNO, while IL-1β from explants correlated with ST tryptophan. We identified less significant correlations between metabolites and these mediators in SF. IL-6 in SF showed an association with succinate and glutamate in SF. While leucine in SF showed negative correlation with TNF, IL-1β, and MMP13 (Supplementary figure 3).

Correlation between metabolites and histological scores also showed a different pattern between ST and SF. While several metabolites from ST were positively associated with inflammation and negatively with fibrosis, we observed the opposite in SF, except for lactate and fumarate that had the same tendency (Supplementary Figure 4). Interestingly, the expression of CD68 in ST was negatively associated with ST glucose and succinate, but positively with ST glycine, fumarate, methionine and lactate. CD68 was also positively associated with acetate, lactate, formate in SF.

3.5. Synovial fluid as predictor of inflammation in synovial tissue

We first compared the SF metabolites by degree of synovitis (using Krenn score) and fibrosis (using picrosirius red score) of the ST. As seen in Supplementary Table 8, concentrations of leucine (86.98 ± 17.24 vs 70.27 ± 16.86, p = 0.04) and tyrosine (48.15 ± 9.07 vs 40.36 ± 8.62, p = 0.06) were lower in SF from samples with high synovitis, while only the concentration of valine (123.06 ± 29.20 vs 146.04 ± 13.53, p = 0.05) was higher in SF from samples with high collagen (Supplementary Table 8).

To further determine whether the SF metabolite profiling was associated with the histological pattern of ST, multivariate approaches were conducted to capture the global picture of metabolite disturbances according to the degree of inflammation. Using an OPLS-DA with all identified metabolites, 58.4% of the total variance across groups explained the separation. A clear separation was observed between the two degrees of synovitis (Fig. 4A), the metabolites responsible for the discrimination were acetoacetate, fumarate, dimethylamine, acetate, succinate, choline, and glutamine. (Fig. 4B). On the other hand, an

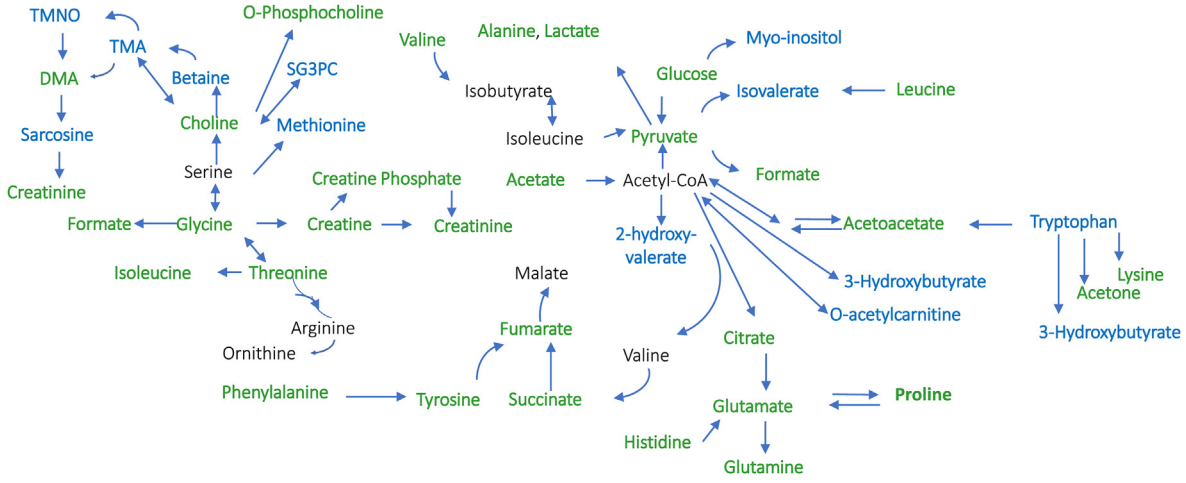

Fig. 2. Map of metabolites identified in synovial tissue and synovial fluid using one dimension proton-Nuclear magnetic resonance (^{1}H NMR). The metabolites found only in synovial tissue are marked in blue, whereas the metabolites identified in both synovial tissue and synovial fluid are marked in green.

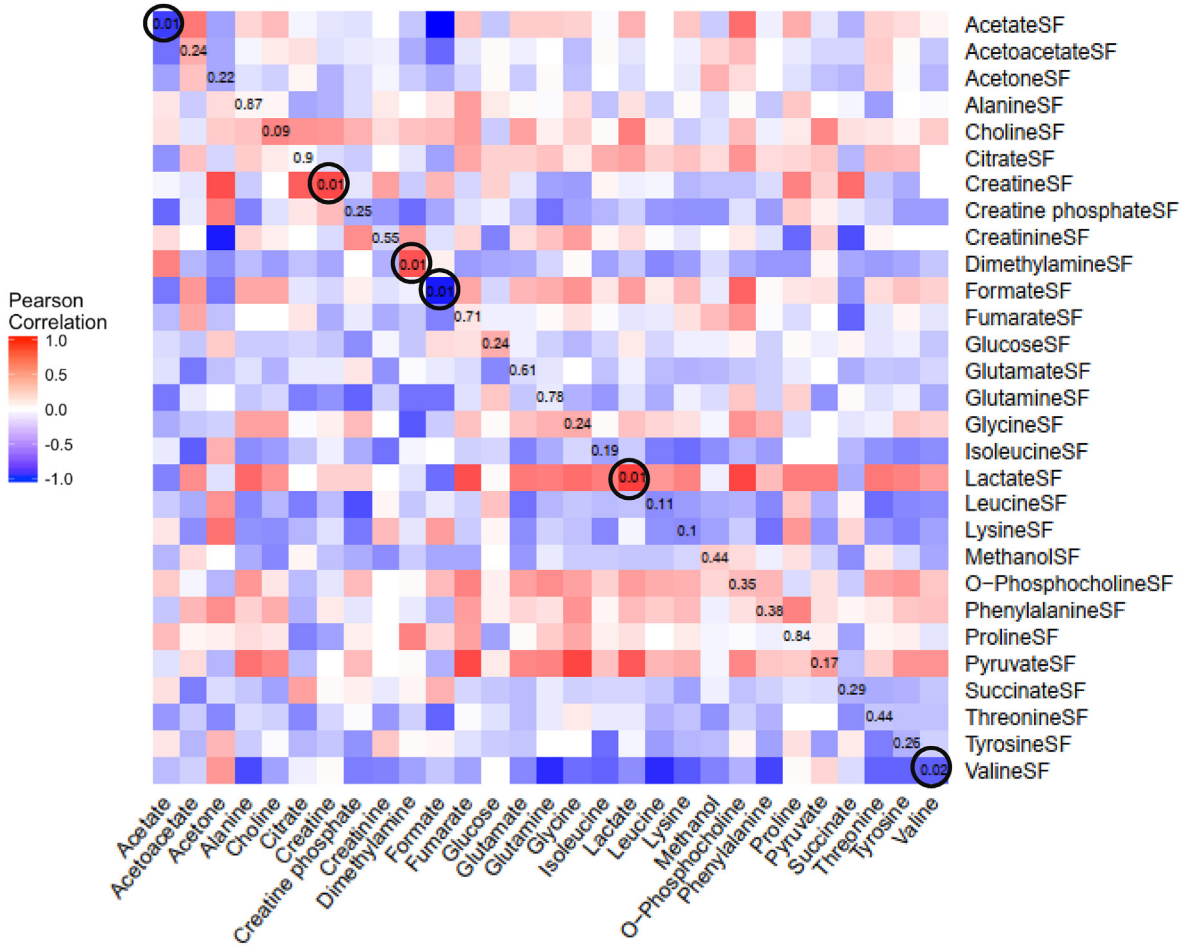

Fig. 3. Pearson correlation of synovial tissue (ST) and synovial fluid (SF) metabolites. The direction of association is showed by color where blue indicates a negative correlation and red indicates a positive correlation and the p value is indicated with the number diagonally on each square indicating the association of metabolites between ST and SF. X axis shows ST metabolites; Y axis shows SF metabolites.

Table 3
Comparison of mediators between inflammation and fibrosis groups quantified in synovial fluid and synovial tissue by ELISA.

SYNOVIAL FLUID						
Mediators	Inflammation		P	Fibrosis		p
	Low synovitis N = 12	High synovitis N = 9		Low collagen N = 9	High collagen N = 12	
TNF	18.43 ± 1.17	19.32 ± 2.16	0.24	19.3 ± 2.2	18.5 ± 1.2	0.59
IL-6	190.8 ± 140.9	639.6 ± 602.6	**0.06**	547.8 ± 597.4	259.6 ± 282.4	0.37
IL-1β	4.62 ± 0.42	9.99 ± 16.84	0.37	10.0 ± 16.8	4.60 ± 0.43	0.34
CXCL2	169.7 ± 163.2	130.7 ± 40.7	0.49	134.6 ± 40.3	166.7 ± 164.0	0.18
CCL2	27.47 ± 48.29	21.06 ± 43.98	0.76	21.1 ± 43.9	27.5 ± 48.3	0.59
MMP13	119.2 ± 109.05	434.1 ± 378.2	**0.04**	332.27 ± 337.4	195.6 ± 266.6	0.46
SYNOVIAL TISSUE						
Mediators	**Inflammation**		**P**	**Fibrosis**		**p**
	Low synovitis N = 14	**High synovitis N = 10**		**Low collagen N = 13**	**High collagen N = 11**	
TNF	23.82 ± 9.32	22.91 ± 12.19	0.84	24.37 ± 12.34	22.49 ± 7.93	0.67
IL-6	33,045 ± 35,699	59,447 ± 52,096	0.15	64,045 ± 49,708	20,411 ± 20,160	**0.01**
IL-1β	7.13 ± 10.68	18.35 ± 39.59	0.43	14.69 ± 34.41	8.06 ± 11.99	0.55
CXCL2	1426 ± 1351	2094 ± 2237	0.38	2208 ± 2065	1077 ± 1108	0.13
CCL2	1319 ± 1632	1166 ± 1206	0.81	1032 ± 1076	1564 ± 1841	0.45
MMP13	85.7 ± 74.8	201.36 ± 409.11	0.40	89.05 ± 77.71	196.98 ± 409.73	0.36

Quantitative variables are expressed in mean ± standard deviation. Student t-test was used to compare quantitative variables. Low synovitis < 5 and high synovitis ≥ 5 according to Krenn score. Low collagen < 2, high collagen ≥ 2 according to picrosirius red staining. TNF: Tumor necrosis factor alpha; IL-6: Interleukin 6; IL-1β: Interleukin 1 beta; CXCL2: C-X-C Motif chemokine ligand 2; CCL2: CC Motif chemokine ligand 2; MMP13: Matrix metallopeptidase 13. Statistical difference was considered when p < 0.05. Concentrations are reported in pg/mL.

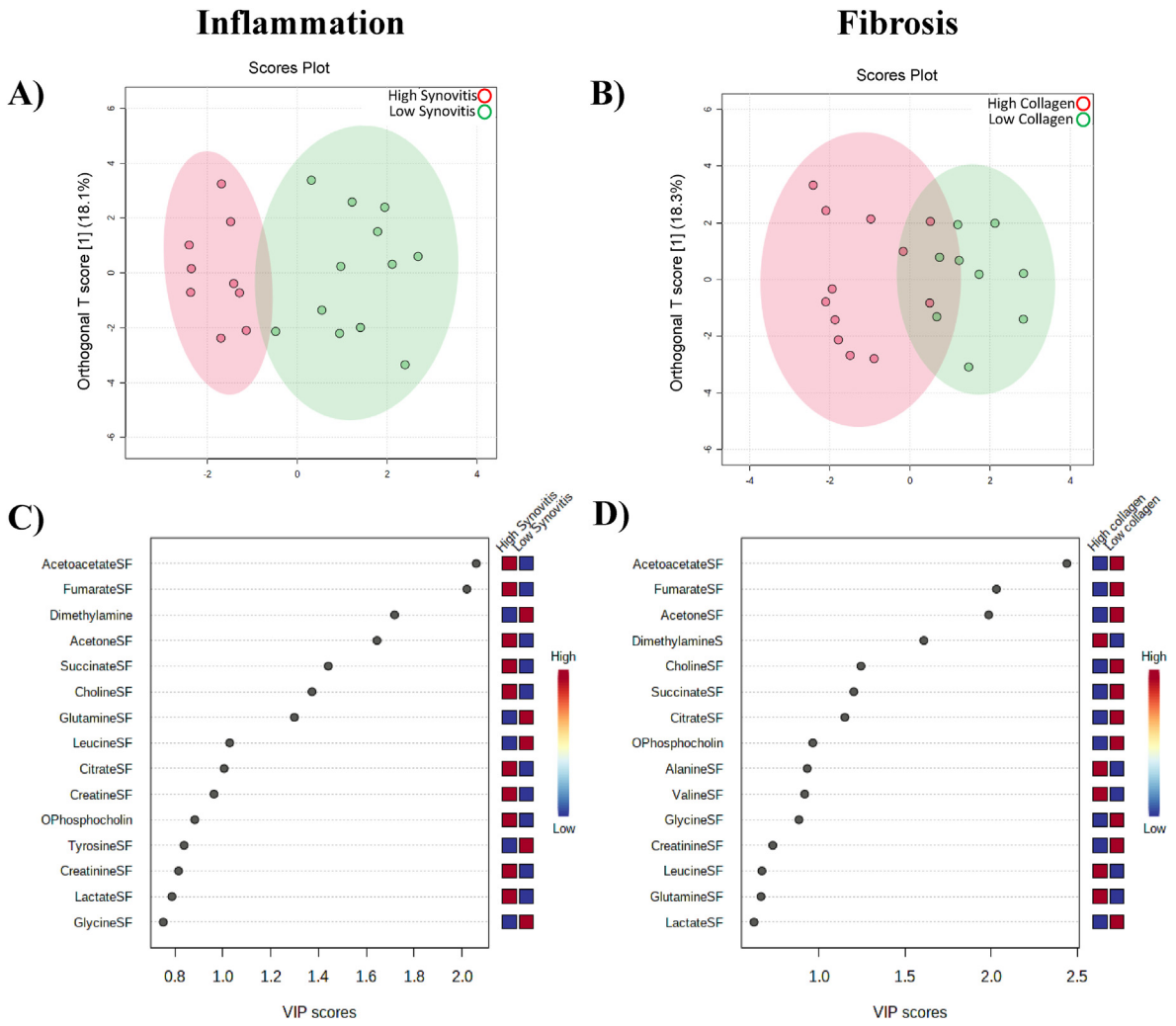

Fig. 4. SF metabolomic profile discriminates between inflammation (A,C) and fibrotic (B,D) scores. Upper figures show orthogonal partial least square-discriminant analysis (OPLS-DA) separation between inflammation (A) and fibrosis (B) groups and bottom figures show the variables important in projection in discriminate inflammation (C) and fibrosis (D), where a variable importance in projection (VIP) score $\geq$1 were considered as important.

overlap existed when divided according to the degree of fibrosis (Fig. 4C). Acetoacetate and fumarate were the most important metabolites in the model (Fig. 4D).

Finally, we built a Random Forest classifier to evaluate the capacity of SF metabolites and mediators to predict the degree of synovitis. There were three SF mediators, namely tyrosine, acetoacetate, and IL-6 that were able to classify the ST samples in high and low synovitis degree with an accuracy of 82%. The ROC performed to evaluate the classifier model yielded an area under curve (AUC) of 0.93, equivalent to a good discriminative ability of the model (Fig. 5).

4. Discussion

In this work, we described the metabolomic profiling of OA synovial samples and identified metabolic changes associated with inflammation. Of interest, IL-6, acetoacetate, and tyrosine in SF predicted high Krenn synovitis scores in ST underscoring that the study of metabolomics and inflammatory mediators in SF can help classify ST by synovial features and also provide information on the potentially activated pathways in the OA synovium. Since one of the main challenges in the management of OA is the lack of effective treatment, due in part to the incomplete understanding of the underlying mechanisms, the study of the metabolomic profile of the OA SF and ST can help better understand the metabolic changes in the OA synovium and identify new therapeutic targets in OA.

Metabolomic profiling from different biofluids has been explored as biomarker of OA and radiographic severity in OA [30]. Plasma levels of succinate, tryptophan, and xanthurenic acid were described as biomarkers to assist the diagnosis of OA [24] and higher concentrations of glutamine, valine, and tyrosine were detected in the synovial fluid of end-stage osteoarthritic knees compared to hips [22]. Also low serum levels of glycine and high levels of arginine were also associated with OA radiographic severity in OA patients [23], while perturbations of glutamine metabolism were found in knee OA patients with inflammation (patients with knee stiffness and positive balloon sign) [20]. However, plasma, serum and urine levels of the metabolites can be influenced by a variety of factors, such as diet, comorbidities, and microbiome, among others. Hence, the metabolomic profile in these biosamples could reflect changes that are not specific to OA.

Here, we observed an increased concentration of several metabolites in ST from OA patients in samples with histological characteristics of inflammation. For instance, TMNO and O-phosphocholine are metabolites derived from choline metabolism, which were related to inflammation [31,32]. Other metabolites such as alanine, fumarate, glutamate, glutamine, glycine, lactate, leucine, lysine, myo-inositol, phenylalanine, and valine were also associated with inflammation in ST. Lactate is a proinflammatory metabolite by reprogramming CD4 T cells, for instance, as consequence of the glycolytic switch of rheumatoid arthritis (RA) FLS [33–35]. Previous studies reported that glutamine/glutamate are also

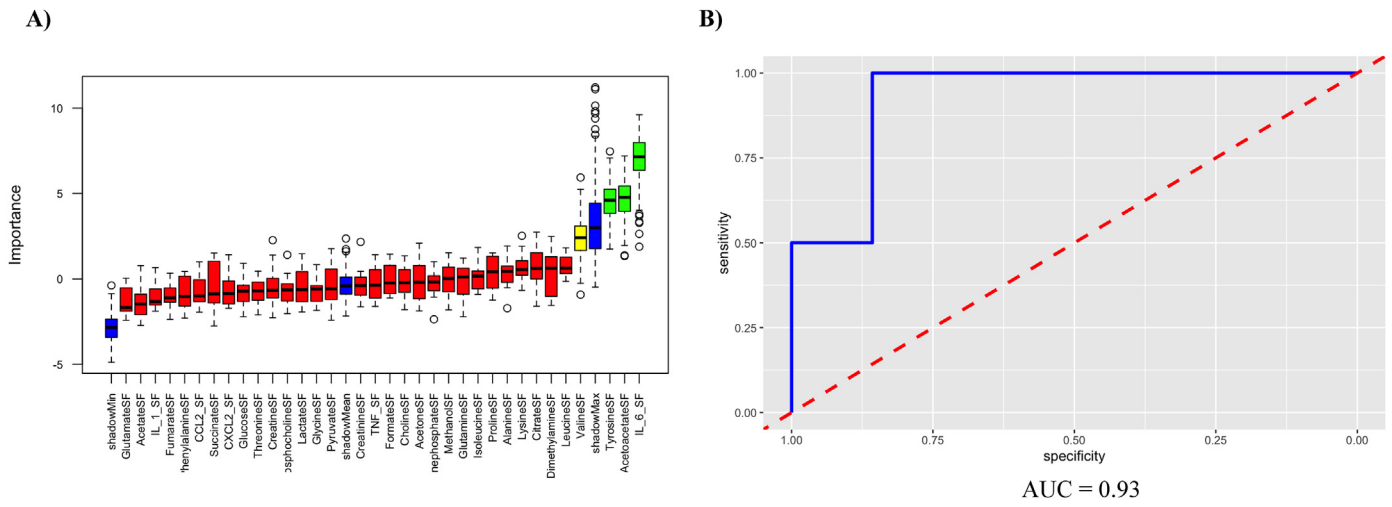

Fig. 5. Receiver operating characteristic curve of the Random Forest model used to assess predictive ability of the synovial fluid (SF) metabolites and mediators to predict degree of synovitis (N = 21). A) Plot of the importance of features (metabolites and cytokines) selected by the Boruta algorithm in relation to the degree of synovitis. Red and yellow features are the ones that were finally rejected, while the green ones (Tyrosine, Acetoacetate and IL-6) are the ones deemed important. B) Receiving receiver operation curve (ROC) of the Random Forest predictive model with an area under curve (AUC) of 0.93.

involved in the aggressive phenotype of RA [36]. Finally, valine and leucine, that are branched-chain amino acids (BCAA), participate, in high concentrations, in ROS generation and inflammation through the activation of NF-KB [37]. Of interest, leucine was decreased in the SF of our inflammatory samples. The high concentration in tissue suggests a probable intake of leucine during inflammation. Low concentrations of small leucine-rich proteoglycans were suggested to participate in the pathogenesis of OA, activating innate immune inflammation and the extracellular collagen network [38]. Of interest, amino acids such as glycine and lysine were described as anti-inflammatory metabolites [39–42]. This observation suggests an increased activity of this pathway in an attempt to suppress inflammation in the joint.

Only a few metabolites had a significant correlation between SF and ST. Acetate, formate, and valine had a negative correlation between SF and ST. These data could reflect the consumption of these metabolites by cells in tissue. On the other hand, lactate, dimethylamine, and creatine positively correlated between ST and SF pointing out to the activation of pathways associated to energy metabolism such as glycolysis and the creatine phosphate pathway [43]. Since SF reflects changes from other joint tissues involved in OA pathogenesis, these results argue with the value of SF as biomarker of ST metabolic changes and emphasize the need of conducting metabolomics in tissue to better understand metabolic drivers of OA synovitis.

Data on the relation between metabolites with synovial fibrosis is lacking. Fibrosis is associated to tissue damage which leads to cellular reprograming of fibroblasts to myofibroblasts [44]. Myofibroblasts are characterized by the secretion of collagen that contributes directly to the formation of fibriosis [44]. We did not phenotype the ST fibroblasts, but interestingly, vimentin levels was associated with inflammation scores and not with fibrotic scores, especially in the synovial sublining, suggesting that fibrosis could be the end result of chronic inflammation as has been described in other diseases [45].

Some metabolites such as proline and glycine were associated with fibrosis in other diseases [46]. Together, glycine, proline, and hydroxyproline (which is produced through posttranslational hydroxylation of collagen proline residues) constitute over half of all amino acids in the primary structure of collagen protein [47]. We found lower concentrations of proline in the group with high collagen. However, as most of the metabolites that were decreased in fibrotic samples were upregulated in the inflammatory samples, our understanding of what drives fibrosis is limited. Of interest, while most of the samples from knees showed high inflammation scores, the samples from hips were more fibrotic. The factors that drive these phenotypes are still unknown. Epigenetic, biomechanical and anatomical factors have been described as contributors [48].

Several metabolites correlated with the expression of CD68 and vimentin. Macrophages and fibroblasts are the most common types of cells in the synovial membrane. In OA, macrophages play a key role in pathogenesis and progression of the disease [5]. We observed an increased expression of CD68 in samples with high synovitis scores, especially in the lining. Activated macrophages have an increased glycolytic influx [49,50]. Interestingly, glucose and succinate in ST were negatively associated with CD68 expression suggesting a consumption of these metabolites by macrophages. Succinate in macrophages triggers the production of IL-1β via hypoxia-inducible factor 1 (HIF1-α) [51,52]. In SF of RA patients, succinate was described to activate macrophages through GRP91 receptor [51]. However, succinate was also proposed as triggering an anti-inflammatory response in macrophages via the same receptor [19,53].

Finally, IL-6, tyrosine and acetoacetate in SF were the metabolites that discriminated between low and high synovitis. IL-6 is a critical proinflammatory cytokine in the inflamed synovium thus it is not surprising to find it as a biomarker of inflammation in SF. Tyrosine is reported to be associated with macrophage activation by its phosphorylation in RA. Interestingly, phenylalanine, which is hydroxylated by phenylalanine 4-hydroxylase (PAH) to tyrosine, and tyrosine works closely with IL-6R which interacts with IL-6 [54]. In addition, tyrosine along with phenylalanine in serum has been implicated in the activation of the immune system in other diseases [55,56]. Finally, β-hydroxybutyrate and acetoacetate have been associated with inflammation by modulating NLRP3 inflammasome, which has been associated to OA pathogenesis [57,58].

There were some limitations in our study. Surgical synovial samples were obtained from suprapatellar area (knee) and from the inferior capsular region (hip) and may not be representative for the entire synovial membrane. However, the process of the sample and the histology criteria was performed following the recommendations by the Outcome Measures in Rheumatoid arthritis Clinical Trials (OMERACT) and the EULAR Synovitis Study Group (ESSG) consensus [8]. In this work, we could not investigate the relationship between histologic and metabolomic changes with clinical data, or the effect of current treatment and comorbidities on inflammation and metabolites. Future studies, with detailed description of clinical outcomes will help validate our results and determine the clinical relevance of the current findings. Lastly, our

study includes only end-stage OA samples from patients who underwent joint replacement. The increased accessibility to ultrasound-guided or arthroscopic synovial biopsies in the outpatient clinic with low adverse effect rate has allowed the characterization of synovia cells in RA. We hope to be able to apply the same techniques to obtain tissue from earlier stages of OA and explore the metabolic alteration at different stages of the disease.

In summary, IL-6, acetoacetate, and tyrosine in SF predicted high Krenn synovitis scores in ST. The study of metabolomics and inflammatory mediators in SF as predictors of inflammation in ST can help classify ST by synovial features and provide information on the potentially activated pathways in the OA synovium. Further in-depth studies are necessary to understand whether or not these changes are driven directly from inflamed tissue or can help identify new therapeutic targets.

Authors contribution

Supervision of overall project: MG. Conception of design: MG. Patient recruitment: NEL, RM. Sample collection: RC, JDM-S. Acquisition of 1H NMR data: JDM-S. Analysis: JDM-S, RC, CL, MG. Interpretation of results: JDM-S, RC, CL, MG. Drafting the manuscript: JDM-S. Revising the manuscript: JDM-S, RC, NEL, MG. All authors read and approved the final manuscript.

Declaration of funding

This work was supported by the National Institute of Health (NIH), United States of America (R01AR073324 to MG, National Institute of Health (NIH), United States of America Diversity Supplement to JDM-S, T32AR064194 to RC, P50 AA011999, P30 DK120515 and D34HP31027 to CL, UCSD School of Medicine Microscopy Core - National Institute of Neurological Disorders and Stroke (NINDS), United States of America P30 NS047101, and University of California San Diego (UCSD), United States of America Clinical and Translational Science Award (CTSA), United States of America - UL1TR001442). CL was also supported by the American Association for the Study of Liver Diseases (AASLD), United States of America Pinnacle Research Award in Liver Disease (8998 GA).

Role of funding source

The funding did not have any role in the study design, in the collection, analysis and interpretation of data; in the writing of the manuscript; or in the decision to submit the manuscript for publication.

Declaration of competing interest

All the authors declare no conflict of interest.

Acknowledgments

Brendan Duggan from UCSD NMR facility of Skaggs School of Pharmacy and Pharmaceutical Science for sample preparation and data acquisition.

Appendix A. Supplementary data

Supplementary data to this article can be found online at https://doi.org/10.1016/j.ocarto.2022.100295.

References

[1] R.F. Loeser, J.A. Collins, B.O. Diekman, Ageing and the pathogenesis of osteoarthritis, Nat. Rev. Rheumatol. 12 (7) (2016) 412–420.
[2] A. Mathiessen, P.G. Conaghan, Synovitis in osteoarthritis: current understanding with therapeutic implications, Arthritis Res. Ther. 19 (1) (2017) 18.
[3] J. Bondeson, S.D. Wainwright, S. Lauder, N. Amos, C.E. Hughes, The role of synovial macrophages and macrophage-produced cytokines in driving aggrecanases, matrix metalloproteinases, and other destructive and inflammatory responses in osteoarthritis, Arthritis Res. Ther. 8 (6) (2006) R187.
[4] J. Bondeson, A.B. Blom, S. Wainwright, C. Hughes, B. Caterson, W.B. van den Berg, The role of synovial macrophages and macrophage-produced mediators in driving inflammatory and destructive responses in osteoarthritis, Arthritis Rheum. 62 (3) (2010) 647–657.
[5] Y. Chen, W. Jiang, H. Yong, M. He, Y. Yang, Z. Deng, et al., Macrophages in osteoarthritis: pathophysiology and therapeutics, Am J Transl Res 12 (1) (2020) 261–268.
[6] H. Zhang, D. Cai, X. Bai, Macrophages regulate the progression of osteoarthritis, Osteoarthritis Cartilage 28 (5) (2020) 555–561.
[7] V. Di Nicola, Degenerative osteoarthritis a reversible chronic disease, Regen Ther 15 (2020) 149–160.
[8] A. Najm, B. Le Goff, C. Orr, R. Thurlings, J.D. Canete, F. Humby, et al., Standardisation of synovial biopsy analyses in rheumatic diseases: a consensus of the EULAR Synovitis and OMERACT Synovial Tissue Biopsy Groups, Arthritis Res. Ther. 20 (1) (2018) 265.
[9] A.C. Stout, M.F. Barbe, C.B. Eaton, M. Amin, F. Al-Eid, L.L. Price, et al., Inflammation and glucose homeostasis are associated with specific structural features among adults without knee osteoarthritis: a cross-sectional study from the osteoarthritis initiative, BMC Muscoskel. Disord. 19 (1) (2018) 1.
[10] J. Sellam, F. Berenbaum, The role of synovitis in pathophysiology and clinical symptoms of osteoarthritis, Nat. Rev. Rheumatol. 6 (11) (2010) 625–635.
[11] A. Mobasheri, M.P. Rayman, O. Gualillo, J. Sellam, P. van der Kraan, U. Fearon, The role of metabolism in the pathogenesis of osteoarthritis, Nat. Rev. Rheumatol. 13 (5) (2017) 302–311.
[12] L. Zheng, Z. Zhang, P. Sheng, A. Mobasheri, The role of metabolism in chondrocyte dysfunction and the progression of osteoarthritis, Ageing Res. Rev. 66 (2021), 101249.
[13] M. Guma, E. Sanchez-Lopez, A. Lodi, R. Garcia-Carbonell, S. Tiziani, M. Karin, et al., Choline kinase inhibition in rheumatoid arthritis, Ann. Rheum. Dis. 74 (7) (2015) 1399–1407.
[14] R. Garcia-Carbonell, A.S. Divakaruni, A. Lodi, I. Vicente-Suarez, A. Saha, H. Cheroutre, et al., Critical role of glucose metabolism in rheumatoid arthritis fibroblast-like synoviocytes, Arthritis Rheumatol. 68 (7) (2016) 1614–1626.
[15] S. Umar, K. Palasiewicz, M.V. Volin, B. Romay, R. Rahat, C. Tetali, et al., Metabolic regulation of RA macrophages is distinct from RA fibroblasts and blockade of glycolysis alleviates inflammatory phenotype in both cell types, Cell. Mol. Life Sci. 78 (23) (2021) 7693–7707.
[16] M.F. Bustamante, P.G. Oliveira, R. Garcia-Carbonell, A.P. Croft, J.M. Smith, R.L. Serrano, et al., Hexokinase 2 as a novel selective metabolic target for rheumatoid arthritis, Ann. Rheum. Dis. 77 (11) (2018) 1636–1643.
[17] E. Sanchez-Lopez, Z. Zhong, A. Stubelius, S.R. Sweeney, L.M. Booshehri, L. Antonucci, et al., Choline uptake and metabolism modulate macrophage IL-1beta and IL-18 production, Cell Metabol. 29 (6) (2019) 1350–13562 e7.
[18] C. Hoyle, J.P. Green, S.M. Allan, D. Brough, E. Lemarchand, Itaconate and fumarate derivatives inhibit priming and activation of the canonical NLRP3 inflammasome in macrophages, Immunology 165 (4) (2022) 460–480.
[19] K.J. Harber, K.E. de Goede, S.G.S. Verberk, E. Meinster, H.E. de Vries, M. van Weeghel, et al., Succinate is an inflammation-induced immunoregulatory metabolite in macrophages, Metabolites 10 (9) (2020).
[20] S. Abdelrazig, C.A. Ortori, M. Doherty, A.M. Valdes, V. Chapman, D.A. Barrett, Metabolic signatures of osteoarthritis in urine using liquid chromatography-high resolution tandem mass spectrometry, Metabolomics 17 (3) (2021) 29.
[21] K.J. Noordwijk, R. Qin, M.E. Diaz-Rubio, S. Zhang, J. Su, L.K. Mahal, et al., Metabolism and global protein glycosylation are differentially expressed in healthy and osteoarthritic equine carpal synovial fluid, Equine Vet. J. 54 (2) (2022) 323–333.
[22] P. Akhbari, M.K. Jaggard, C.L. Boulange, U. Vaghela, G. Graca, R. Bhattacharya, et al., Differences in the composition of hip and knee synovial fluid in osteoarthritis: a nuclear magnetic resonance (NMR) spectroscopy study of metabolic profiles, Osteoarthritis Cartilage 27 (12) (2019) 1768–1777.
[23] K. Tootsi, K. Vilba, A. Martson, J. Kals, K. Paapstel, M. Zilmer, Metabolomic signature of amino acids, biogenic amines and lipids in blood serum of patients with severe osteoarthritis, Metabolites 10 (8) (2020).
[24] Z. Huang, Z. He, Y. Kong, Z. Liu, L. Gong, Insight into osteoarthritis through integrative analysis of metabolomics and transcriptomics, Clin. Chim. Acta 510 (2020) 323–329.
[25] R. Altman, E. Asch, D. Bloch, G. Bole, D. Borenstein, K. Brandt, et al., Development of criteria for the classification and reporting of osteoarthritis. Classification of osteoarthritis of the knee. Diagnostic and Therapeutic Criteria Committee of the American Rheumatism Association, Arthritis Rheum. 29 (8) (1986) 1039–1049.
[26] V. Krenn, L. Morawietz, G.R. Burmester, R.W. Kinne, U. Mueller-Ladner, B. Muller, et al., Synovitis score: discrimination between chronic low-grade and high-grade synovitis, Histopathology 49 (4) (2006) 358–364.
[27] C.M. Lopez De Padilla, M.J. Coenen, A. Tovar, R.E. De la Vega, C.H. Evans, S.A. Muller, Picrosirius red staining: revisiting its application to the qualitative and quantitative assessment of collagen type I and type III in tendon, J. Histochem. Cytochem. 69 (10) (2021) 633–643.
[28] R. Lattouf, R. Younes, D. Lutomski, N. Naaman, G. Godeau, K. Senni, et al., Picrosirius red staining: a useful tool to appraise collagen networks in normal and pathological tissues, J. Histochem. Cytochem. 62 (10) (2014) 751–758.
[29] A.R. Crowe, W. Yue, Semi-quantitative determination of protein expression using immunohistochemistry staining and analysis: an integrated protocol, Bio Protoc 9 (24) (2019) e3465.

[30] S.A.A. Showiheen, A.R. Sun, X. Wu, R. Crawford, Y. Xiao, R.M. Wellard, et al., Application of metabolomics to osteoarthritis: from basic science to the clinical approach, Curr. Rheumatol. Rep. 21 (6) (2019) 26.
[31] R. Coras, A. Kavanaugh, T. Boyd, D. Huynh, K.A. Lagerborg, Y.J. Xu, et al., Choline metabolite, trimethylamine N-oxide (TMAO), is associated with inflammation in psoriatic arthritis, Clin. Exp. Rheumatol. 37 (3) (2019) 481–484.
[32] R. Volchenkov, M. Dung Cao, K.B. Elgstoen, G.L. Goll, K. Eikvar, O. Bjorneboe, et al., Metabolic profiling of synovial tissue shows altered glucose and choline metabolism in rheumatoid arthritis samples, Scand. J. Rheumatol. 46 (2) (2017) 160–161.
[33] M.A. Neveu, N. Beziere, R. Daniels, C. Bouzin, A. Comment, J. Schwenck, et al., Lactate production precedes inflammatory cell recruitment in arthritic ankles: an imaging study, Mol. Imag. Biol. 22 (5) (2020) 1324–1332.
[34] R. Haas, J. Smith, V. Rocher-Ros, S. Nadkarni, T. Montero-Melendez, F. D'Acquisto, et al., Lactate regulates metabolic and pro-inflammatory circuits in control of T cell migration and effector functions, PLoS Biol. 13 (7) (2015), e1002202.
[35] V. Pucino, M. Certo, V. Bulusu, D. Cucchi, K. Goldmann, E. Pontarini, et al., Lactate buildup at the site of chronic inflammation promotes disease by inducing CD4(+) T cell metabolic rewiring, Cell Metabol. 30 (6) (2019) 1055–10574 e8.
[36] A. Torres, B. Pedersen, I. Cobo, R. Ai, R. Coras, J. Murillo-Saich, et al., Epigenetic regulation of nutrient transporters in rheumatoid arthritis fibroblast-like synoviocytes, Arthritis Rheumatol. 74 (7) (2022) 1159–1171.
[37] O. Zhenyukh, E. Civantos, M. Ruiz-Ortega, M.S. Sanchez, C. Vazquez, C. Peiro, et al., High concentration of branched-chain amino acids promotes oxidative stress, inflammation and migration of human peripheral blood mononuclear cells via mTORC1 activation, Free Radic. Biol. Med. 104 (2017) 165–177.
[38] G.X. Ni, Z. Li, Y.Z. Zhou, The role of small leucine-rich proteoglycans in osteoarthritis pathogenesis, Osteoarthritis Cartilage 22 (7) (2014) 896–903.
[39] J. Cheng, J.C. Tang, M.X. Pan, S.F. Chen, D. Zhao, Y. Zhang, et al., l-lysine confers neuroprotection by suppressing inflammatory response via microRNA-575/PTEN signaling after mouse intracerebral hemorrhage injury, Exp. Neurol. 327 (2020), 113214.
[40] N. Zhang, X. Su, K. Xu, [Comparison of the application between circular stapler and linear stapler in Billroth II(anastomosis of distal gastrectomy], Zhonghua Wei Chang Wai Ke Za Zhi 21 (2) (2018) 201–205.
[41] Z. Zhong, M.D. Wheeler, X. Li, M. Froh, P. Schemmer, M. Yin, et al., L-Glycine: A novel antiinflammatory, immunomodulatory, and cytoprotective agent, Curr. Opin. Clin. Nutr. Metab. Care 6 (2) (2003) 229–240.
[42] N.K. Khanna, B.R. Madan, Anti-inflammatory activity of DL-valine, Indian J. Exp. Biol. 16 (7) (1978) 834–836.
[43] H. Taegtmeyer, J.S. Ingwall, Creatine–a dispensable metabolite? Circ. Res. 112 (6) (2013) 878–880.
[44] A. Maglaviceanu, B. Wu, M. Kapoor, Fibroblast-like synoviocytes: role in synovial fibrosis associated with osteoarthritis, Wound Repair Regen. 29 (4) (2021) 642–649.
[45] I. Chimenti, S. Sattler, G. Del Monte-Nieto, E. Forte, Editorial: fibrosis and inflammation in tissue pathophysiology, Front. Physiol. 12 (2021), 830683.
[46] R.B. Hamanaka, G.M. Mutlu, The role of metabolic reprogramming and de novo amino acid synthesis in collagen protein production by myofibroblasts: implications for organ fibrosis and cancer, Amino Acids 53 (12) (2021) 1851–1862.
[47] K.H. Bradley, S.D. McConnell, R.G. Crystal, Lung collagen composition and synthesis. Characterization and changes with age, J. Biol. Chem. 249 (9) (1974) 2674–2683.
[48] M. Hall, M. van der Esch, R.S. Hinman, G. Peat, A. de Zwart, J.G. Quicke, et al., How does hip osteoarthritis differ from knee osteoarthritis? Osteoarthritis Cartilage 30 (1) (2022) 32–41.
[49] A.K. Jha, S.C. Huang, A. Sergushichev, V. Lampropoulou, Y. Ivanova, E. Loginicheva, et al., Network integration of parallel metabolic and transcriptional data reveals metabolic modules that regulate macrophage polarization, Immunity 42 (3) (2015) 419–430.
[50] A. Viola, F. Munari, R. Sanchez-Rodriguez, T. Scolaro, A. Castegna, The metabolic signature of macrophage responses, Front. Immunol. 10 (2019) 1462.
[51] A. Littlewood-Evans, S. Sarret, V. Apfel, P. Loesle, J. Dawson, J. Zhang, et al., GPR91 senses extracellular succinate released from inflammatory macrophages and exacerbates rheumatoid arthritis, J. Exp. Med. 213 (9) (2016) 1655–1662.
[52] G.M. Tannahill, A.M. Curtis, J. Adamik, E.M. Palsson-McDermott, A.F. McGettrick, G. Goel, et al., Succinate is an inflammatory signal that induces IL-1beta through HIF-1 alpha, Nature 496 (7444) (2013) 238–242.
[53] N. Keiran, V. Ceperuelo-Mallafre, E. Calvo, M.I. Hernandez-Alvarez, M. Ejarque, C. Nunez-Roa, et al., SUCNR1 controls an anti-inflammatory program in macrophages to regulate the metabolic response to obesity, Nat. Immunol. 20 (5) (2019) 581–592.
[54] C. Blanchetot, N. De Jonge, A. Desmyter, N. Ongenae, E. Hofman, A. Klarenbeek, et al., Structural mimicry of receptor interaction by antagonistic interleukin-6 (IL-6) antibodies, J. Biol. Chem. 291 (26) (2016) 13846–13854.
[55] P. Sirnio, J.P. Vayrynen, K. Klintrup, J. Makela, T. Karhu, K.H. Herzig, et al., Alterations in serum amino-acid profile in the progression of colorectal cancer: associations with systemic inflammation, tumour stage and patient survival, Br. J. Cancer 120 (2) (2019) 238–246.
[56] C. Murr, T.B. Grammer, A. Meinitzer, M.E. Kleber, W. Marz, D. Fuchs, Immune activation and inflammation in patients with cardiovascular disease are associated with higher phenylalanine to tyrosine ratios: the ludwigshafen risk and cardiovascular health study, J. Amino Acids 2014 (2014), 783730.
[57] Y. Onizawa, T. Katoh, R. Miura, K. Konda, T. Noguchi, H. Iwata, et al., Acetoacetate is a trigger of NLRP3 inflammasome activation in bovine peripheral blood mononuclear cells, Vet. Immunol. Immunopathol. 244 (2022), 110370.
[58] Y.H. Youm, K.Y. Nguyen, R.W. Grant, E.L. Goldberg, M. Bodogai, D. Kim, et al., The ketone metabolite beta-hydroxybutyrate blocks NLRP3 inflammasome-mediated inflammatory disease, Nat Med 21 (3) (2015) 263–269.